Cross-Equatorial Flow and Seasonal Cycle of Precipitation over South America

HUI WANG AND RONG FU

School of Earth and Atmospheric Sciences, Georgia Institute of Technology, Atlanta, Georgia

(Manuscript received 6 July 2001, in final form 10 December 2001)

ABSTRACT

The relationship between South American precipitation and cross-equatorial flow over the western Amazon is examined using the 15-yr (1979–93) European Centre for Medium-Range Weather Forecasts (ECMWF) reanalysis dataset. A meridional wind index, the V index, is constructed to represent the variability of the cross-equatorial flow, based on area-averaged (5°S–5°N, 65°–75°W) daily 925-hPa meridional winds. The V index displays large submonthly, seasonal, and interannual variabilities, and correlates well with precipitation over South America. Two circulation regimes are identified, that is, a southerly regime and a northerly regime. Linear regression shows that when the V index is southerly, precipitation is mainly located to the north of the equator. When the V index is northerly, precipitation shifts toward the Amazon basin and subtropical South America. The V index is predominately southerly in austral winter and northerly in summer. The onset (demise) of the Amazon rainy season is led by an increase in the frequency of the northerly (southerly) V index. The relation between the V index and upper-level circulation is consistent with the seasonal cycle of the South American monsoon circulation. Hence, the V index is a good indicator for precipitation change over tropical and subtropical South America.

The singular value decomposition (SVD) analysis suggests that the V-index-related variation represents 92% of the total covariance between the low-level meridional wind and precipitation over South America. It also represents 37% of the seasonal variance of precipitation. On the seasonal timescale, the V index appears to correlate well with the meridional migration of the Hadley cell globally. On submonthly timescales, the change of V index is not correlated with the meridional wind over the adjacent oceans except in the South Atlantic convergence zone, suggesting a control by more localized and higher-frequency dynamic processes. The SVD analysis also suggests that during spring and fall precipitation changes over the equatorial eastern Amazon are associated with the seasonal variations of sea surface temperature in the Pacific and the Atlantic Oceans.

1. Introduction

The annual amount of precipitation in tropical and subtropical South America is largely influenced by the length of the wet season (Liebmann et al. 1999; Marengo et al. 2001) and may vary as much as 40% (Kousky 1988), which dwarfs any known annual variations in solar radiation. Hence, a reliable seasonal prediction of precipitation over South America is very much needed for assisting local agriculture, managing the ecosystem, and generating hydroelectricity. However, considerable uncertainties exist in current predictions due to a limited understanding of complex spatial and temporal variations in precipitation and the rapid onset of the wet season.

The seasonal variation of South American precipitation is characterized by a wet season over the Amazon basin and subtropics in austral summer and a dry season in winter, as shown in Fig. 1. The onset of the wet season starts in the equatorial western Amazon (Fig. 1a) and then spreads quickly to the east and the southeast. This preliminary stage lasts about one month during spring (Horel et al. 1989) and is followed by a wet season with abundant rainfall across the Amazon basin (Fig. 1b). During fall, regions of large precipitation shrink in size and migrate gradually toward the equator (Fig. 1c), indicating the end of the Amazon rainy season. In the dry season (Fig. 1d), occurrences of maximum rainfall are mainly confined north of the equator. Clearly, the seasonal cycle of South American precipitation involves a significant meridional migration of rainfall between south and north of the equator. There are also some distinctions in seasonal variation of precipitation over the equatorial eastern and western Amazon. In both summer and winter, the equatorial Amazon serves as a divide for wet and dry conditions on each side of the equator. There is moderate rainfall in both the eastern and western Amazon during these two seasons (Figs. 1b and 1d). In spring, when the onset of the wet season occurs, the equatorial western Amazon experiences a significant increase in precipitation. In contrast, this is the time when the equatorial eastern Amazon is having its driest season (Fig. 1a). During fall, the seasonal mi-

Corresponding author address: Dr. Hui Wang, School of Earth and Atmospheric Sciences, Georgia Institute of Technology, 221 Bobby Dodd Way, Atlanta, GA 30332-0340.
E-mail: huiwang@eas.gatech.edu

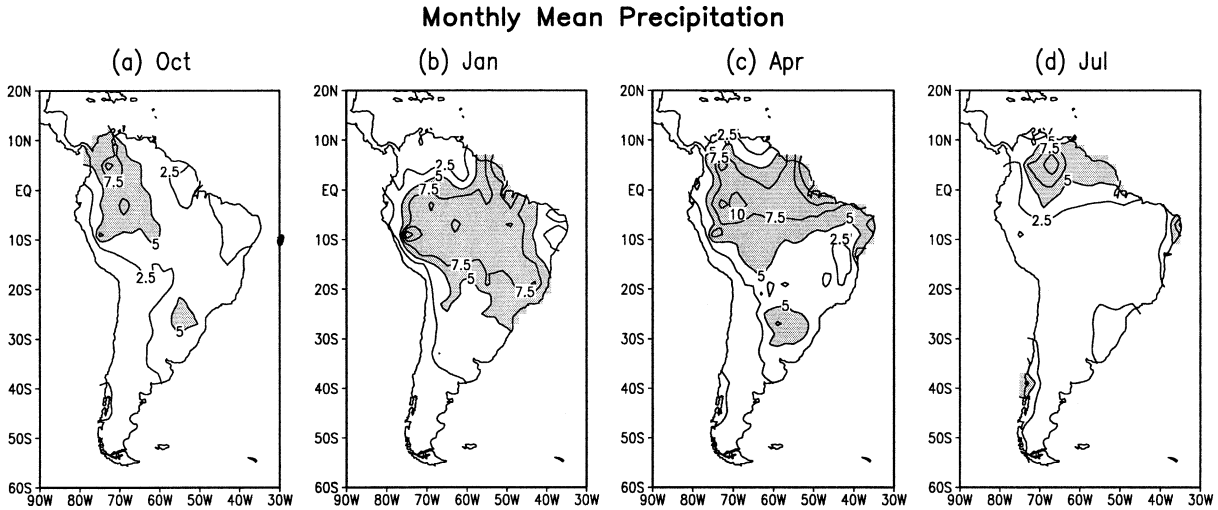

FIG. 1. Observed climatological monthly mean precipitation over South America for (a) Oct, (b) Jan, (c) Apr, and (d) Jul in the period of 1979–93. Contour interval is 2.5 mm day^{-1}. Rainfalls greater than 5 mm day^{-1} are shaded.

gration of rainfall crosses the equator, leading to a peak in precipitation over both equatorial eastern and western Amazon (Fig. 1c). The seasonal changes in precipitation over the eastern Amazon are thus larger than these changes over the western Amazon.

South America has been traditionally regarded as a nonmonsoon climate regime. Zhou and Lau (1998), however, have demonstrated that the main features of the seasonal reversal of the large-scale circulation over South America resemble those of a monsoon system when the annual mean winds are removed. Other previous observations also revealed monsoonlike features. For example, Horel et al. (1989) have shown that the Bolivian high builds up rapidly during the onset. Li and Fu (2002, manuscript submitted to *J. Climate*, hereafter LF) have found that the onset of the wet season in South America resembles that of the Asian monsoon (Krishnamurti et al. 1998) in several ways. In particular, the stretching of an atmospheric column converts low-level potential energy into upper-level divergent kinetic energy, and the interaction between divergent and rotational winds at the upper level quickly transforms the divergent kinetic energy into rotational kinetic energy. Consequently, an upper-level anticyclonic vorticity center is initiated. Although these studies have characterized the transition of the large-scale thermal and dynamic conditions during the onset, what triggers this transition and whether a precursor of the onset can be found remain unanswered. The analysis of radiosonde profiles (Fu et al. 1999) has suggested that the onset of the wet season is initiated by increased moisture due to transport above the planetary boundary layer and decreased temperatures at the top of the boundary layer. However, the large-scale processes responsible for these changes have not been adequately examined. A clarification of these issues will provide critical information for improving prediction of the onset of the wet season over South America.

Seasonal variation of Amazon rainfall is contributed by changes in individual precipitation systems, which are associated with the changes of atmospheric circulation on synoptic and intraseasonal timescales (Park and Schubert 1993; Kousky and Kayano 1994). Even within the wet season, dry and wet spells on submonthly timescales are well documented (Nogues-Paegle and Mo 1997; Garreaud and Wallace 1998). In fact, the evidences presented in this paper suggest that the precise date of the wet season onset may largely depend on these submonthly activities. The wet and dry seasons are likely brought on by more frequent and persistent occurrences of circulation patterns similar to those during the wet and dry intraseasonal periods, as a result of modulations in the atmospheric circulation caused by external forcing, such as solar radiation and sea surface temperatures (SSTs) in the adjacent oceans. Hence, understanding the relationship between precipitation and large-scale circulation patterns on submonthly timescales could help us to determine the causes of highly variable seasonal distribution of precipitation over South America, which is fundamentally driven by relatively regular external solar forcing.

In this paper, we apply a monsoon index developed for the Asian monsoon (Lu and Chan 1999) to identify the area that most effectively captures the seasonal reversal of the circulation over South America. As we will show in this paper, a reversal of meridional wind across the equator in the western Amazon leads to the onset of the wet season and also correlates well with the latitudinal shift of precipitation over South America on submonthly timescales. The objectives of this study are to characterize the relationship between the low-level cross-equatorial flow and precipitation over South

America and to explore the potential for using this cross-equatorial flow as a predictor of South American precipitation. These objectives will be approached by examining the seasonal and submonthly variations of the cross-equatorial flow and establishing their relationship to the seasonal cycle of precipitation over South America using a 15-yr reanalysis dataset and empirical methods. The primary concern is to identify precipitation patterns that are associated with two atmospheric circulation regimes, that is, the cross-equatorial southerly wind regime and northerly wind regime. In the next section, the dataset and statistical techniques are described. A meridional wind index (V index) representing the variation of the cross-equatorial flow is defined in section 3. The relationships between the V index and South American precipitation on seasonal and submonthly timescales are analyzed in sections 4 and 5, respectively. Conclusions are given in section 6.

2. Data and methods

The data used in this study consist of precipitation, three-dimensional atmospheric wind fields, specific humidity, and relative humidity. They are taken from the European Centre for Medium-Range Weather Forecasts (ECMWF) reanalysis (ERA) on a 2.5° lat × 2.5° lon grid and at 17 pressure levels. The original data were recorded 4 times daily at 0000, 0600, 1200, and 1800 UTC, respectively, over a 15-yr period (1979–93). Although there is a bias toward a wetter condition over the eastern Amazon in this dataset, the precipitation from ERA captures well the observed seasonal migration of precipitation over South America (not shown), and it is thus employed in this study. The seasonal variation of precipitation is a low-frequency phenomenon with timescales of about a month and longer. A field experiment suggested that atmospheric convection accounts for a significant amount of precipitation over the Amazon basin (Greco et al. 1990). The seasonal changes in rainfall are likely a manifestation of the changes in frequency and intensity of the atmospheric convection, which is generated by the variations of the synoptic-scale atmospheric circulation. Therefore, in addition to monthly mean data, daily mean data are also used to resolve the relationship between precipitation and the atmospheric circulation associated with convection. In this study, we choose the data from January, April, July, and October to represent the austral summer, fall, winter, and spring, respectively. The data from these months capture the major seasonal features. The monthly mean precipitation data on a 2° × 2° grid from the Climate Anomaly Monitoring System (CAMS) developed at the National Centers for Environmental Prediction (NCEP) are adopted to illustrate the seasonal cycle of precipitation (Fig. 1) and to compare it with composite rainfall patterns associated with different atmospheric circulation regimes. Monthly mean SSTs are also used to examine the influence of adjacent oceans on South American precipitation, which are taken from the NCEP-reconstructed SST dataset (Smith et al. 1996) on a 2° × 2° grid.

Three statistical methods are used to measure associations between atmospheric circulation and precipitation. The first one is the correlative analysis, in which a temporal correlation coefficient is calculated between the time series of precipitation and the V index. This simple technique is capable of revealing a linear relationship between the two variables. The normalized correlation coefficients, however, provide no information on the actual rates of change in precipitation and circulation. Composites based on linear regressions against the V index are thus used to obtain the rates of change in both precipitation and circulation and their spatial distributions associated with fluctuations in the V index. The third method is the singular value decomposition (SVD; Bretherton et al. 1992), which is able to objectively identify pairs of spatial patterns describing the maximum temporal covariance between precipitation and the atmospheric circulation.

3. Cross-equatorial flow and the V index

Over the equatorial South America, through the gap between the Andes and the mountain complex to the east, a narrow band of strong northerly winds is often observed in the lower troposphere. The wind speed can be as high as 15 m s^{-1} in austral summer months. Figure 2a shows the typical wind pattern at 925 hPa. The meridional wind is a dominant component. The vertical profiles of wind speed (Fig. 2b) display low-level wind maximums and an apparent nocturnal intensification, which are the two major features of low-level jet (LLJ; Stensrud 1996). In company with the cross-equatorial northerly LLJ, convection and precipitation occur frequently over the Amazon basin and subtropical South America. No study has so far systematically examined this recurrent cross-equatorial flow or its relation to South American precipitation.

The implications of this low-level flow for the monsoonlike seasonal variation of circulation over South America are explored using a unified monsoon index for the east Asian monsoon by Lu and Chan (1999). They simply used climatological monthly mean surface meridional wind and added together all southerly winds and all northerly winds. The minimum value of the two summations is defined as the monsoon index. A large monsoon index thus indicates a strong reversal of the meridional wind occurring during the annual cycle. We applied this monsoon index to the South American region using 925-hPa monthly mean meridional winds, at which level both the cross-equatorial flow (Fig. 2) and the meridional moisture transport (not shown) are relatively strong. As shown in Fig. 3, the region where the strong cross-equatorial northerly winds occur frequently during summer (Fig. 2, 5°S–5°N, 65°–75°W) experiences a relatively strong reversal of meridional wind in

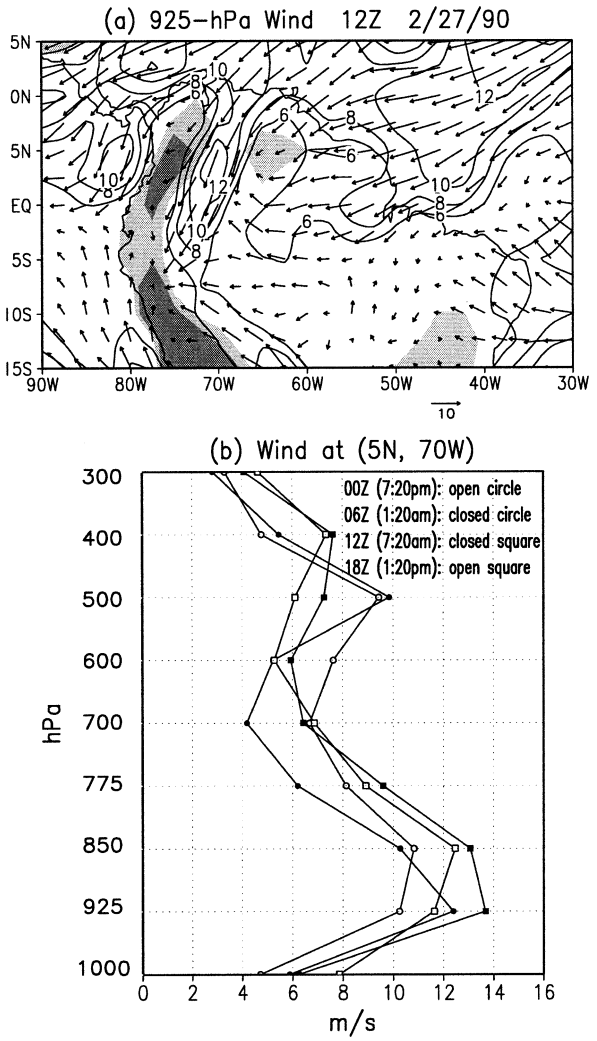

FIG. 2. (a) 925-hPa wind (vectors) and isotach (contours) at 1200 UTC and (b) vertical profiles of horizontal wind speed at (5°N, 70°W) for 0000, 0600, 1200, and 1800 UTC of 27 Feb 1990. Contour interval is 2 m s^{-1} in (a). Light (dark) shading indicates elevations over 500 (1000) m. Local time is indicated in parentheses in (b).

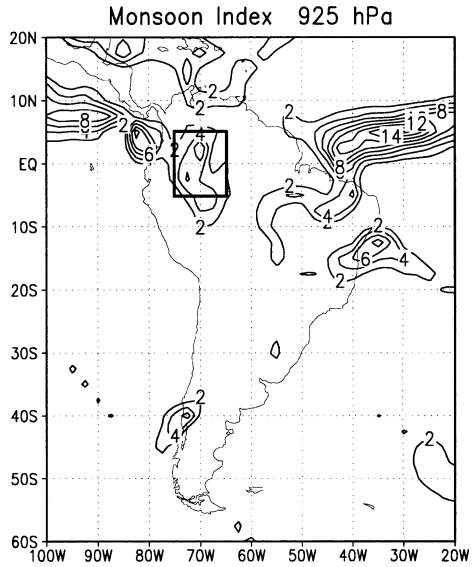

FIG. 3. 925-hPa monsoon index, as defined by Lu and Chan (1999). Contour interval is 2 m s^{-1}. The box at the equator indicates the domain of (5°S–5°N, 65°–75°W).

the annual cycle. The monsoon index is generally small over the rest of the South American continent. The area with moderate magnitudes on the subtropical east coast is associated with the South Atlantic convergence zone (SACZ). Over the tropical oceans, the reversal of meridional wind is also strong in the Pacific and Atlantic intertropical convergence zones (ITCZs). The monsoon index suggests that the reversal of the cross-equatorial flow over the western Amazon may be representative of the variation of the South American monsoon circulation.

To better represent the variability of the cross-equatorial flow over the equatorial western Amazon, a meridional wind index, the V index (VI), is constructed by averaging the 925-hPa meridional winds over the domain of maximum monsoon index (5°S–5°N, 65°–75°W) using the daily mean data. The 15-yr daily VI is shown in Fig. 4 for each month. In October, both southerly and northerly winds are observed. At the end of the austral spring (November, not shown), the northerly events are more frequent than the southerly. In January, the cross-equatorial flow is dominated by the northerly regime, and in July, it is dominated by the southerly regime. In additional to the seasonal variation, VI also displays strong interannual and submonthly variations. There are significant peaks at 5–14 days in the power spectrum of the 15-yr daily VI (not shown). Figure 5 summarizes the monthly statistics of the 15-yr daily VI. The frequency of occurrence for northerly events is 70%–95% in summer and 25%–40% in winter (Fig. 5a). Consistently, the climatological monthly mean VI is northerly in summer and southerly in winter (Fig. 5b). The intensity of monthly averaged northerly (southerly) flow is strongest in summer (winter) and exceeds 2 m s^{-1}, as shown in Fig. 5c.

4. Relationship between V index and precipitation on a seasonal timescale

To explore a possible connection between the cross-equatorial flow and the seasonal variation of precipitation over South America, Fig. 6a shows the correlation of observed precipitation from CAMS with VI, using *monthly* mean data from all months over the 15-yr period (180 months). Both long-term annual mean precipitation and VI were removed prior to the calculation. The correlation in Fig. 6 thus primarily reflects their relationship by way of seasonal variations. Areas of significant positive correlations are found north of the equator and those of significant negative correlations

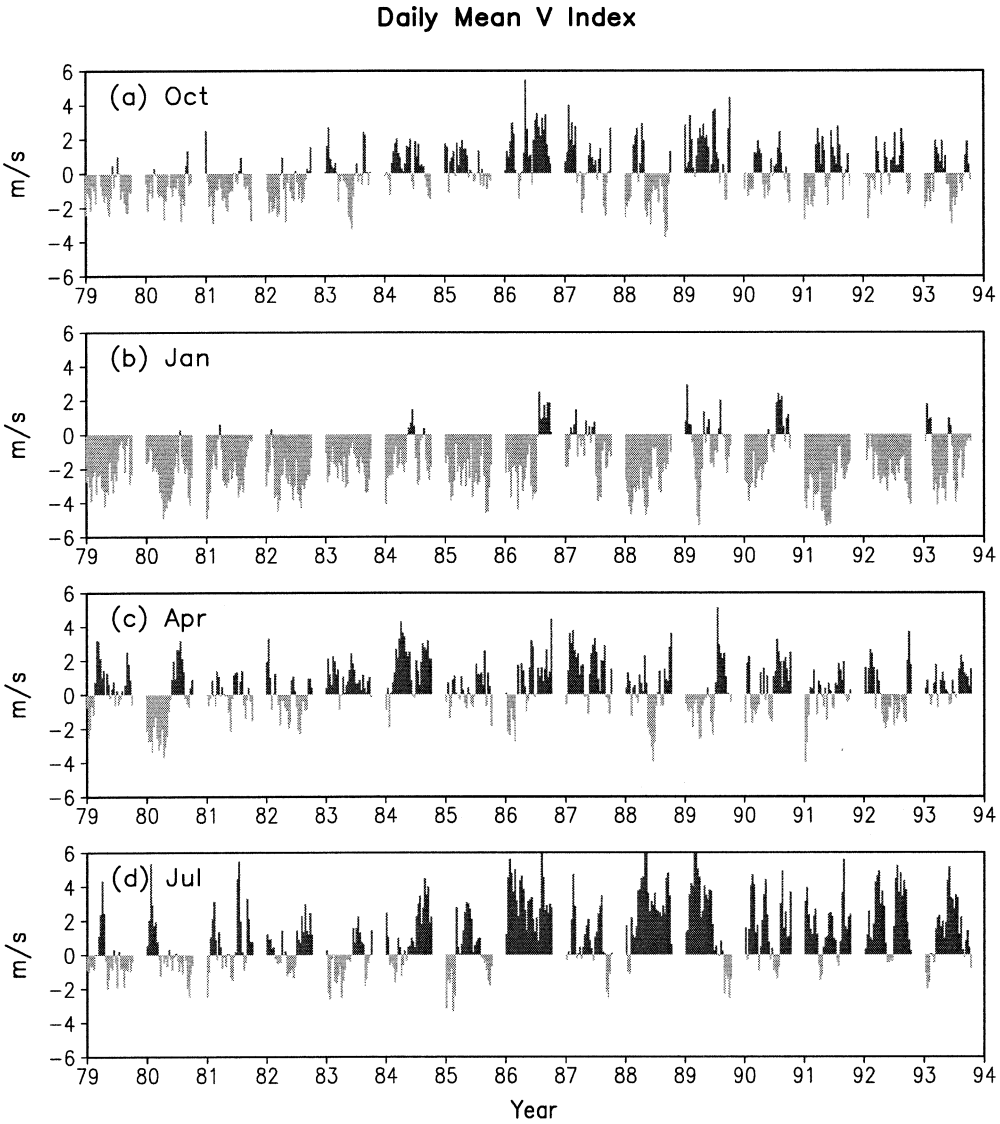

FIG. 4. Time series of 925-hPa daily mean meridional winds averaged over (5°S–5°N, 65°–75°W), the V index, for (a) Oct, (b) Jan, (c) Apr, and (d) Jul from 1979 to 1993. Dark (light) bars indicate southerly (northerly) winds. The data are not sequential in time, in that Oct of 1979 is right next to Oct of 1980. Spaces are thus placed between jumps from one year to the next.

south of the equator in the Tropics and subtropics. This suggests that a wet condition north of the equator and a dry condition over most of the Southern Hemisphere continent are associated with the southerly regime. In the northerly regime, more precipitation appears over the Amazon basin and subtropics. The results are consistent with the seasonal variations of both precipitation and VI shown in Figs. 1 and 5. The correlation pattern with VI for precipitation from ERA (Fig. 6b) is similar to that for observed precipitation (Fig. 6a). The resemblance provides confidence in the usefulness of precipitation data from ERA.

The importance of the cross-equatorial flow to the seasonal variation of South American precipitation and its linkage to the global-scale circulation are examined by an SVD analysis, based on cross-covariance matrices of monthly mean 925-hPa meridional wind and CAMS monthly mean precipitation over South America for the 15-yr period (1979–93, 180 months). As in the correlation analysis, both climatological annual mean meridional wind and precipitation are subtracted from the data. Table 1 lists the statistics of the first two SVD modes, including the percentage of squared covariance explained by each mode, the temporal correlation between each pair of expansion coefficients, and the variances in individual fields that are explained by each mode. Together the two modes account for 97% of squared covariance between the two fields, and the cor-

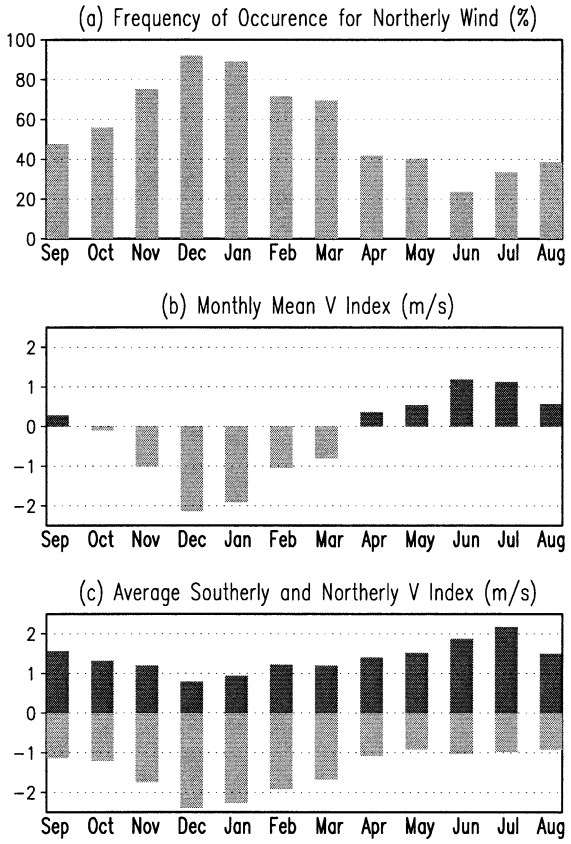

FIG. 5. (a) Frequency of occurrence for northerly winds in the V index, (b) monthly mean values of the V index, and (c) monthly mean southerly and northerly V index averaged over 1979–93. Dark (light) bars indicate southerly (northerly) winds.

responding components explain 47% of the meridional wind variance and 50% of the precipitation variance over South America, respectively, regarding their climatological annual means. The spatial patterns of the two SVD modes are presented using the heterogeneous correlation (Wallace et al. 1992). Although only meridional winds over the South American continent are used in the analysis, the heterogeneous correlation maps for the wind field are shown in a larger domain to demonstrate linkage to global-scale variations.

The first SVD mode explains 92% of squared covariance between meridional wind and precipitation. The heterogeneous correlation patterns are shown in Figs. 7a and 7b. The wind pattern itself explains 38% of the total variance of the monthly mean wind (Table 1). This mode is characterized by large negative correlations over the entire Tropics. Relatively strong correlations tongue into the gap between the Andes and the mountains to the east in equatorial South America, where the cross-equatorial flow occurs. Some positive correlations are found in the extratropics. The first SVD mode of precipitation, which explains 37% of the total precipitation variance, is virtually identical to the pattern of correlations between precipitation and VI (Fig. 6a), except for opposite signs. The relationship between the cross-equatorial wind and South American precipitation is well defined by the first SVD mode. In addition, the changes in the cross-equatorial flow east of the Andes are linked to a global-scale variation in the low-level meridional winds over the entire Tropics. The second SVD mode explains 5% of the squared covariance between meridional wind and precipitation. The wind pattern (Fig. 7c) displays coherent negative correlations over the tropical oceans and positive correlations near the South Pacific convergence zone and SACZ. The weak correlation in the equatorial western Amazon suggests that the second mode reflect the variations that are unrelated to the V index. The precipitation pattern (Fig. 7d) shows large positive correlations over the equatorial eastern Amazon between 5°S and 5°N. This mode relates the eastern Amazon precipitation to the seasonal changes of SST in both the Pacific and the Atlantic, as shown below.

In order to highlight the seasonality in the relationship between the low-level meridional wind and the South American precipitation, the normalized SVD time series are averaged over the 15 years for each month, as shown in Fig. 8. In the first mode, the time series of both meridional wind and precipitation display a well-defined annual cycle with peaks in summer and valleys in winter. It is suggested that the wet (dry) season over the Amazon basin and extratropics is associated with cross-equatorial northerly (southerly) wind anomalies that occur not only to the east of the Andes but also throughout the entire Tropics in summer (winter). In fact, these meridional winds, as well as VI, constitute the low branch of the Hadley circulation. The annual march of meridional wind slightly leads the precipitation variation, especially in the transitional seasons. A similar feature has also been found by LF that shows the occurrence of cross-equatorial northerly winds over the western Amazon leads the onset of the Amazon wet season. The cross-equatorial flow thus may possess predictive value for the onset and end of the Amazon rainy season. The second mode shows a 3-month phase lag with respect to the first mode. The equatorial eastern Amazon is relatively wet during fall and dry during spring (Fig. 7d). In contrast, the precipitation over the equatorial western Amazon has smaller seasonal changes. This is consistent with the evolution of monthly mean precipitation (Fig. 1). Fu et al. (2001) have shown that the seasonal variations in precipitation over the eastern Amazon in austral spring and fall are strongly influenced by the seasonal changes of SST in both the Pacific and the Atlantic, whereas precipitation in the equatorial western Amazon is relatively insensitive to the SST changes. Since the second SVD mode shows large precipitation variation over the equatorial eastern Amazon during spring and fall, we calculated both lead and lag correlations between SST and the precipitation time series of the second SVD mode, as shown in Fig. 9. There are significant positive (negative) correlations

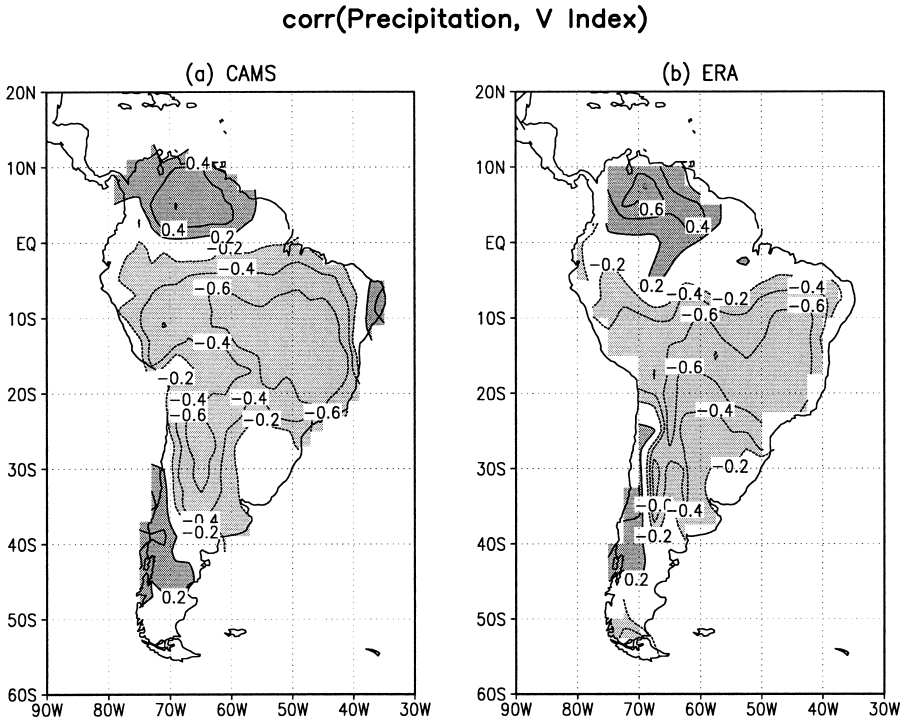

FIG. 6. Correlations of monthly mean precipitation (a) from CAMS and (b) from ERA with monthly mean V index over the period of 1979–93. Contour interval is 0.2. Zero contours are omitted and negative contours are dashed. Dark (light) shading indicates values of positive (negative) correlations exceeding 0.2.

in the southern (northern) oceans, except in Fig. 9e. The correlations when SST leads precipitation by 1–2 months (Figs. 9a and 9b) are stronger than the simultaneous correlation (Fig. 9c) and those when SST lags by 1–2 months (Figs. 9d and 9e). This suggests an SST forcing to the eastern Amazon precipitation. The correlation patterns indicate that more (less) precipitation in the eastern Amazon in austral fall (spring) is associated with warmer (colder) SST in the southern oceans and colder (warmer) SST in the northern oceans, consistent with the seasonal cycles of both SST and eastern Amazon precipitation during spring and fall (Figs. 1 and 7–9). The second SVD thus supports the model results of Fu et al. (2001) that seasonal changes of SST in the adjacent oceans significantly influence the eastern Amazon precipitation in the equinox seasons.

The SVD analysis effectively separates the seasonal cycle of South American precipitation into two major components: the seasonal variation associated with the Hadley circulation across the equator during summer and winter and the influence of SST in the adjacent oceans during spring and fall. The V-index-related variation is the largest contributor to the total seasonal variation of precipitation and dominates the covariance between the meridional wind and precipitation over South America (92%), as represented by the first SVD mode.

TABLE 1. Statistics of the two leading SVD modes between 925-hPa meridional wind and precipitation over South America.

SVD mode	Squared covariance	Temporal correlation	925-hPa wind variance	Precipitation variance
Mode 1	92%	0.89	38%	37%
Mode 2	5%	0.74	9%	13%

5. Relationship between V index and precipitation on submonthly timescales

In addition to the large seasonal variability, the V index also has strong fluctuations on submonthly timescales (Fig. 4). Whether the submonthly variation of precipitation is related to that of VI provides a further test of the relationship between VI and precipitation over South America found by way of seasonal variations. Figure 10 shows the linear regression coefficient of precipitation against VI, based on the 15-yr *daily* mean data for October, January, April, and July, respectively. It indicates the rate of change in precipitation associated with a 1 m s^{-1} increase in VI. In general, the spatial patterns of the regression coefficient using daily mean data for individual months are similar to the correlation pattern with monthly mean data (Fig. 6). Specifically, there are large positive coefficients to the north of the equator and negative coefficients to the south. Therefore, the relationship between cross-equatorial flow and precipitation on submonthly timescales

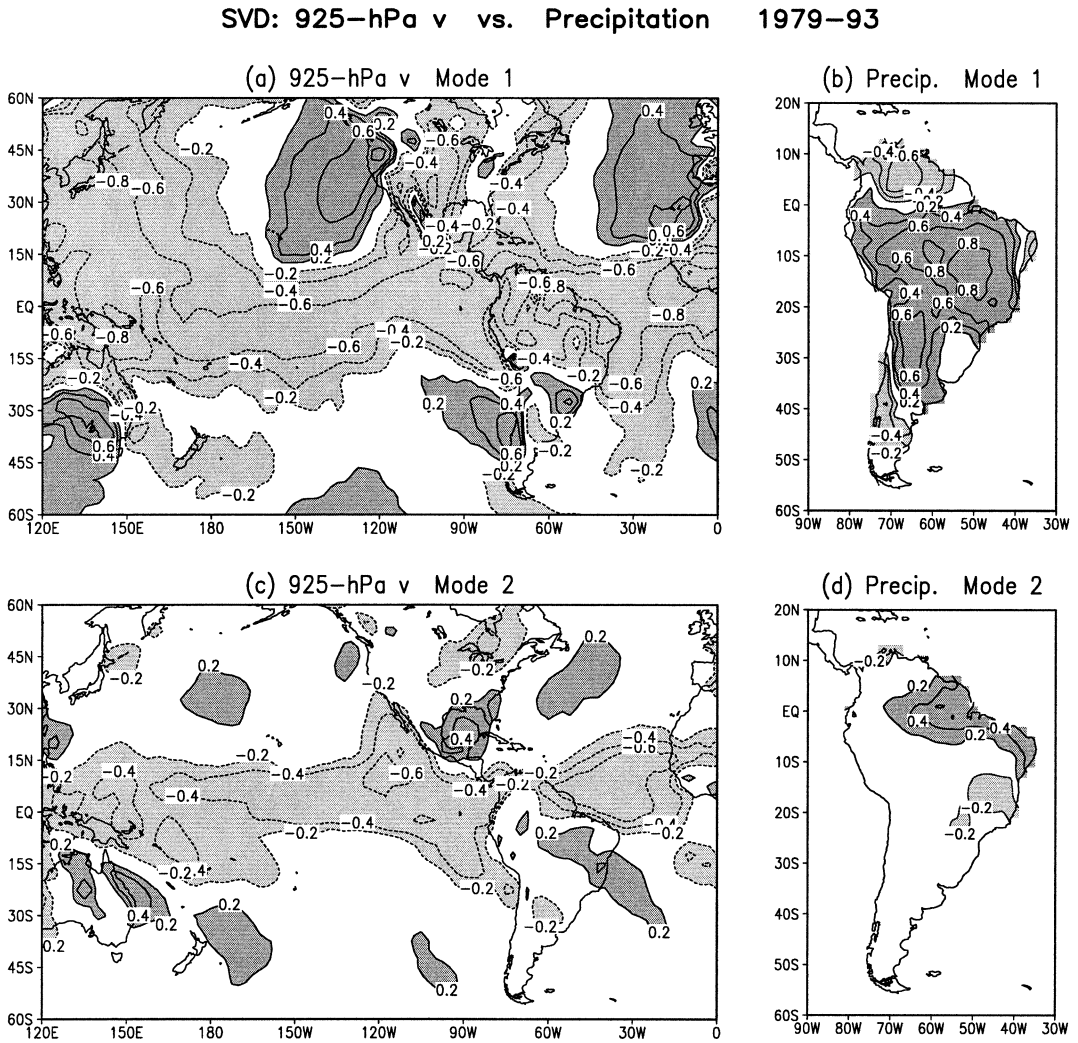

FIG. 7. Heterogeneous correlations of the first two SVD modes between 925-hPa meridional wind and CAMS precipitation over South America, using 15-yr monthly mean data (180 months). Contour interval is 0.2. Zero contours are omitted and negative contours are dashed. Dark (light) shading indicates values of positive (negative) correlations exceeding 0.2.

is similar to that on the seasonal timescale. Associated with a 1 m s^{-1} increase (decrease) in VI, precipitation can be increased (decreased) by 1–3 mm day^{-1} north of the equator and decreased (increased) by 0.5–2.5 mm day^{-1} over the Amazon basin and subtropics. Distinctions also exist among different seasons. Both positive and negative regression coefficients in July, the dry season, are weaker than those in other months. The negative regression coefficients in eastern Brazil in January, the peak of the wet season, are the strongest. In January, negative coefficients are also found over the SACZ region and positive coefficients over southern Brazil. In contrast, the negative coefficients in other months extend farther to the extratropics of South America and the South Atlantic.

Figure 11 shows composite patterns of precipitation, 925-hPa wind, and moisture divergence fields for each month, which are constructed based on the linear regressions of the 15-yr daily mean data, associated with 2 m s^{-1} (southerly regime) and -2 m s^{-1} (northerly regime) in VI, respectively. This magnitude of VI is a mean value in summer and winter (Fig. 5c) and also representative for spring and fall (Fig. 4). In each month, there is an elongated rainfall band over the equatorial Pacific and Atlantic, respectively. The precipitation is weak and close to the equator in January and April, but strong and away from the equator in July and October, characterizing the seasonal migration of ITCZs. Within the same season, there is no significant difference in precipitation pattern over the tropical oceans between the southerly and northerly regimes. Over South America, however, precipitation exhibits large differences between the two circulation regimes.

In the southerly regime (Figs. 11a,c,e,g) there are two

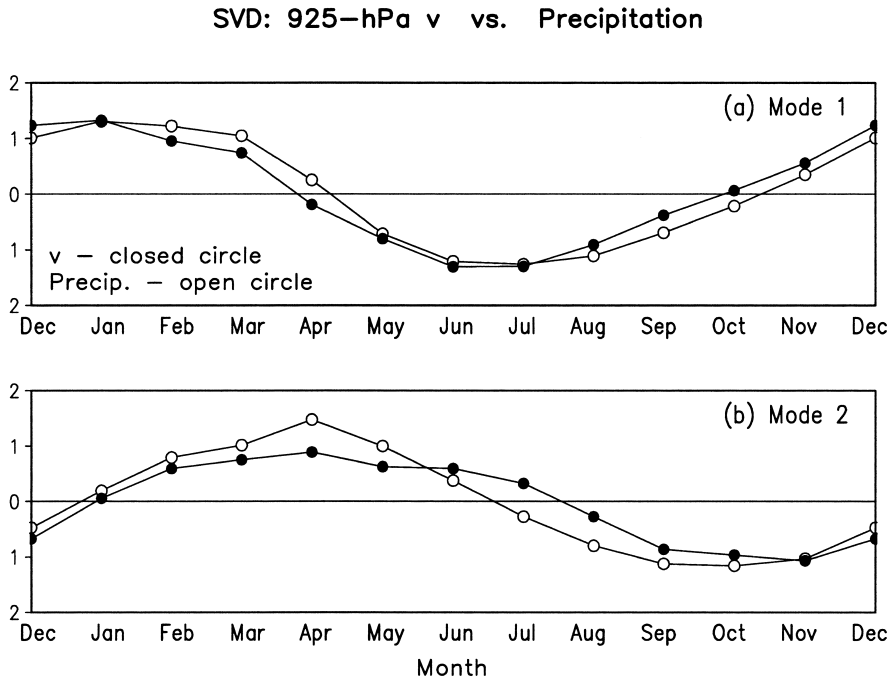

FIG. 8. Time series of the first two SVD modes averaged over the 15-yr period (1979–93) for each month of a year.

centers of maximum rainfall in the equatorial South America. One is located in the northwest of the continent and the other in the eastern Amazon. Both are coincidental with strong low-level moisture convergence in these regions. The moisture convergence in the northwest primarily results from a southeasterly flow across the equator. When the Atlantic ITCZ is away from the equator in July and October (Figs. 11a and 11g), the moisture convergence in the eastern Amazon is largely due to winds from the southern Atlantic Ocean. When the Atlantic ITCZ is near the equator as in January and April (Figs. 11c and 11e), the moisture convergence related to greater precipitation is contributed by winds coming from both sides of the equator. This indicates a seasonal change of moisture sources for convergence in the eastern Amazon. Over the subtropics, the anticyclonic circulation associated with the subtropical high is weak near the east coast of South America. The winds blowing from the subtropical Atlantic split into two branches, one blowing toward the equatorial Amazon and the other toward extratropical South America. These features become more apparent in the 925-hPa streamlines (not shown). Consequently, subtropical South America experiences low-level divergence and a dry condition. It is noted that there is a relatively strong northerly flow east of the Andes between 20° and 35°S, the region where LLJs are known to occur frequently (Stensrud 1996; Paegle 1998). The low-level northerly flow is strongest in January and likely responsible for heavy precipitation in southern Brazil (Fig. 11c). This is consistent with the facts that LLJs are strongly associated with deep convection (Stensrud 1996), and mesoscale convective complexes are often observed in southern Brazil during summer (Velasco and Fritsch 1987).

In the northerly regime (Figs. 11b,d,f,h) a common feature in all seasons is the southward shift of precipitation. Particularly, the maximum precipitation and strong moisture convergence disappear in the tropical northwest. The area north of the equator is relatively dry. In western South America, the cross-equatorial northerly flow penetrates all the way to the extratropics. Due to the blocking effect by the Andes, there is a moisture convergence zone along the east slope of the Andes. In the east, the precipitation pattern varies with season. The increase in precipitation south of the equator in the northerly regime is most robust in January (Fig. 11d). Associated with 2 m s^{-1} of northerly VI, precipitation exceeds 10 mm day^{-1} in the eastern Amazon and the land portion of SACZ. It also increases by 5–10 mm day^{-1} throughout the western Amazon and subtropical South America. The northerly flow penetrates from the equator to the central Amazon and the subtropics. The easterly flow from the Atlantic Ocean converges in the eastern Amazon and the subtropics, consistent with the heavy precipitation in the same region. In July, precipitation is confined to the east coast of extratropical South America. A high frequency of cyclogenesis to the southwest of the subtropical high in the South Atlantic (Gan and Rao 1991) may be responsible for this. In April (Fig. 11f) and October (Fig. 11b), precipitation increases mostly to the east of the Andes between 20° and 35°S.

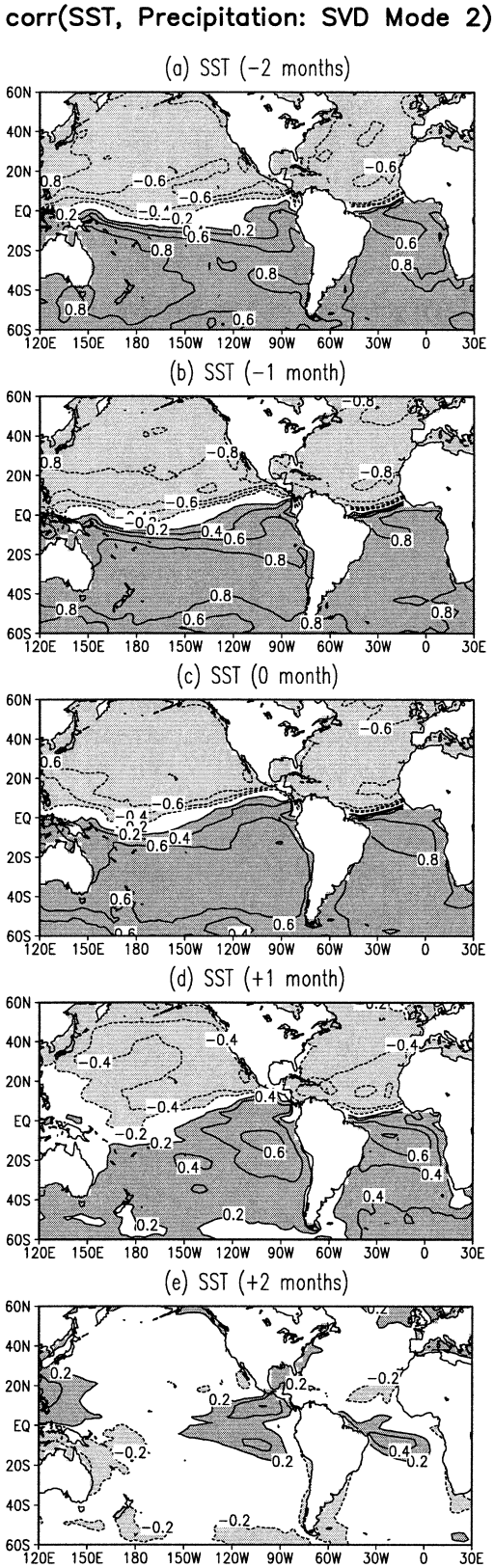

The moisture convergence in these regions is mainly contributed by northerly flow from the Amazon and easterly flow farther to the south. The subtropical LLJs also exist in the northerly regime. They are located between 10° and 25°S and are much stronger than those in the southerly regime. This may indicate a possible influence of the cross-equatorial flow on the subtropical LLJs.

A comparison between the observed monthly mean precipitation and composites suggests that the seasonal variation of South American precipitation is likely related to the variations of the cross-equatorial flow on submonthly timescales. The onset of the wet season (Fig. 1a) is likely associated with an increased frequency of the northerly events during spring (Figs. 5a, 11a, and 11b). In summer, heavy precipitation over the Amazon basin and subtropical South America is related to the prevailing northerly regime (Figs. 5 and 11d). During fall, diminishing rainfall in the subtropics and a migration of precipitation toward the equator are closely related to a transition from the northerly regime to the southerly (Figs. 5, 11e, and 11f). In the winter season, the observed maximum precipitation north of the equator (Fig. 1d) is mainly associated with the prevailing southerly regime (Figs. 5 and 11g). The results illustrate the seasonal cycle of South American precipitation accompanying the changes in direction of the cross-equatorial wind and frequency of southerly and northerly events. We also examined lead and lag relationships between precipitation and the cross-equatorial wind. Figure 12 shows the linear regression coefficient of precipitation against the 15-yr daily VI, for VI leading and lagging precipitation by 2 days, respectively. The negative regression coefficients along the east of the Andes when VI leads precipitation (Figs. 12a,c,e,g) are stronger than those when VI lags precipitation (Figs. 12b,d,f,h) in all seasons. This suggests that the precipitation over the western Amazon is primarily driven by the cross-equatorial northerly wind. Since the Amazon rainy season starts from this region during spring (Fig. 1a; Marengo et al. 2001), the V index may be a useful predictor for the onset of the Amazon wet season. In January, large negative coefficients are found in the eastern Amazon in both VI leading and lagging precipitation cases (Figs. 12c and 12d), indicating a positive feedback between the cross-equatorial northerly flow and convection over the eastern Amazon in summer. Details of the cause and effect relationship are under investigation.

The Bolivian high has been recognized as a predominant feature in the upper troposphere associated with

←

FIG. 9. Lead and lag correlations between SST and the precipitation time series of the second SVD mode, using 15-yr monthly mean data (180 months). Correlation maps are shown for SST leading precipitation by (a) 2 months, (b) 1 month, (c) 0 months, and lagging by (d) 1 month and (f) 2 months. Contours and shadings are the same as in Fig. 7.

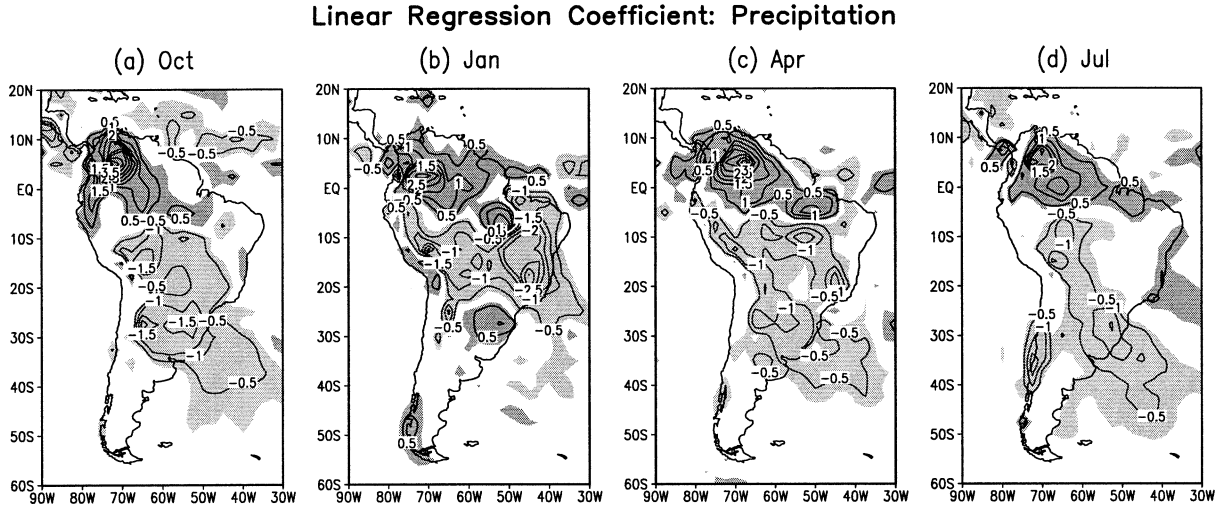

FIG. 10. Linear regression coefficient for (a) Oct, (b) Jan, (c) Apr, and (d) Jul daily precipitation associated with the 15-yr daily mean V index. Contour interval is 0.5 mm day^{-1} (m s^{-1})$^{-1}$. Zero contours are omitted. Dark (light) shading indicates positive (negative) coefficients exceeding 0.25 mm day^{-1} (m s^{-1})$^{-1}$.

the onset and evolution of the Amazon wet season. The relationship between the upper-level circulation and VI is also examined by using the linear regression of 15-yr daily mean 200-hPa winds against VI. Figure 13 presents the upper-level circulation patterns associated with the southerly and northerly regimes, respectively. In October, in the southerly regime (Fig. 13a), the circulation is characterized by a center of upper-level divergence over the north side of the equator (0°–10°S), which can be seen more clearly in the streamline field (not shown). In the northerly regime (Fig. 13b), a well-defined Bolivian high is built up over the southern Amazon (5°–15°S). The circulation pattern in Fig. 13a (13b) is very similar to both the composite of 200-hPa winds prior to (after) the onset (Horel et al. 1989) and the circulation during the premonsoon (monsoon development) phase (Zhou and Lau 1998). In January, the upper-level anticyclone in the northerly regime is substantially intensified and shifted to the subtropics (Fig. 13d), which is the canonical circulation pattern in the wet season and referred to as the mature stage of the South American monsoon in Zhou and Lau (1998). In the southerly regime system, the January circulation is characterized by a low over the east coast and a high over the west coast. A similar circulation pattern is indeed observed during the wet season, when the central Amazon experiences less precipitation (Rickenbach et al. 2002, their Fig. 5a). In April, the anticyclone is weakened and shifted away from the Altiplano Plateau in the northerly regime (Fig. 13f), similar to that in the monsoon-withdraw phase (Zhou and Lau 1998). In the southerly regime, it is almost deteriorated, corresponding to the post-monsoon phase (Zhou and Lau 1998). In July, when the low-level southerly winds prevail at the equator, upper-level westerly winds dominate over the subtropical South America (Fig. 13g), a major feature of the winter climatology. Occasionally, when a northerly flow occurs, there is a center of weak upper-level divergence over the central Amazon (Fig. 13h), which is related to convection in the same region (Fig. 11h). Evidently, the establishment of the Bolivian high is associated with the transition from the southerly regime to the northerly during spring. Its enhancement and decay are related to strong persistence of the northerly regime in summer and an increased number of southerly events in fall, respectively. This suggests a close relationship between the variations of the low-level cross-equatorial wind and upper-level circulation.

Deep convection over the subtropical South America in relation to VI is accessed by using vertical cross sections and data from January, during which time convection is usually strongest. Figure 14 shows the wind field, relative humidity, and precipitation at 15°S associated with different VI, based on the linear regressions. In the subtropics, over the central and eastern parts of the continent, sinking motion is associated with the southerly regime (Fig. 14a), while rising motion is associated with the northerly regime (Figs. 14c and 14d). The relative humidity of the lower troposphere increases with the cross-equatorial northerly wind. The moist air brought from the equatorial Atlantic by the northerly flow increases the probability of precipitation over these regions. On the other hand, both upward motion and relative humidity over western subtropical South America are relatively insensitive to the change in the cross-equatorial wind. It is likely related to the blocking effect of the Andes. At 15°S the Andes peaks above 4 km and has a northwest–southeast orientation. Thus, it can effectively block low-level northeasterly winds prevailing in the region. The results suggest a significant oscillation and distinctions in the atmospheric convection between the east and the west of sub-

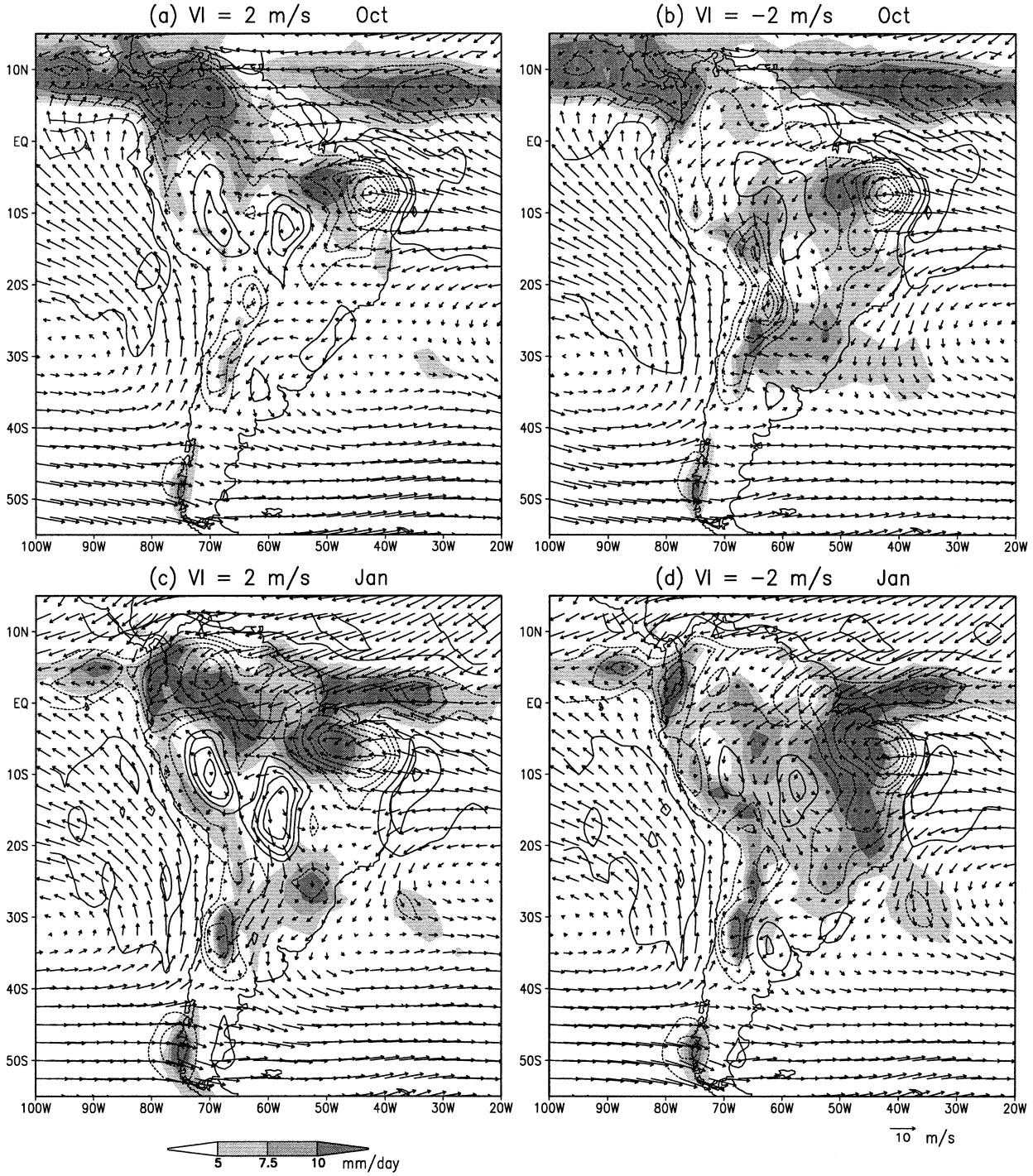

FIG. 11. Regression patterns of precipitation (shadings), 925-hPa horizontal wind (vectors) and divergence of 925-hPa moisture flux (contours) associated with (a),(c),(e),(g) 2 m s^{-1} and (b),(d),(f),(h) −2 m s^{-1} fluctuations in the V index for (a),(b) Oct, (c),(d) Jan, (e),(f) Apr, and (g),(h) Jul. Contour interval is 0.5×10^{-4} g kg^{-1} s^{-1}, with negative values dashed. Zero contours are omitted. Light, dark and darker shadings indicate precipitation over 5, 7.5, and 10 mm day^{-1}, respectively.

tropical South America in relation to the southerly and northerly regimes.

A recent analysis of observational data from a field experiment for the January–February 1999 period (Rickenbach et al. 2002; Petersen et al. 2002) revealed that convection in Rondonia, Brazil (11°S, 62°W) is strongly affected by different large-scale circulation patterns, that is, the low-level easterly and westerly winds.

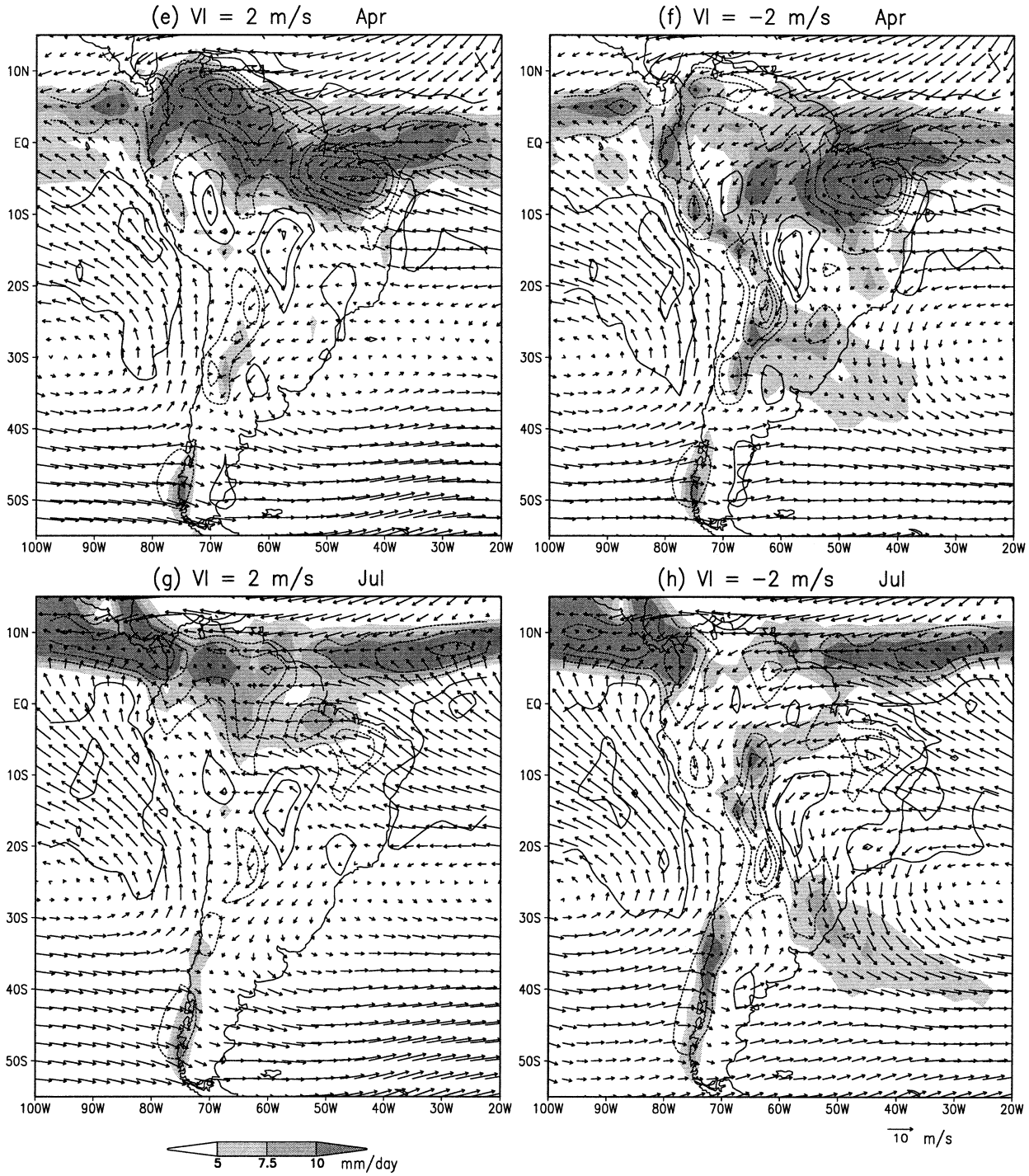

FIG. 11. (*Continued*)

It is interesting to know whether the subtropical easterly and westerly wind regimes are related to the cross-equatorial flow or are independent of VI. Figure 15 shows January 925-hPa meridional and zonal wind changes corresponding to a shift in VI from 2 to -2 m s^{-1}, based on the linear regression. The anomalous northerly winds at the equator and southerly winds in higher latitudes of South America (Fig. 15a) produce a strong low-level convergence over the Amazon basin and subtropics. Associated with the northerly (southerly) flow at the equator, there is an increase (decrease) in zonal wind over the Amazon basin and subtropics (Fig. 15b).

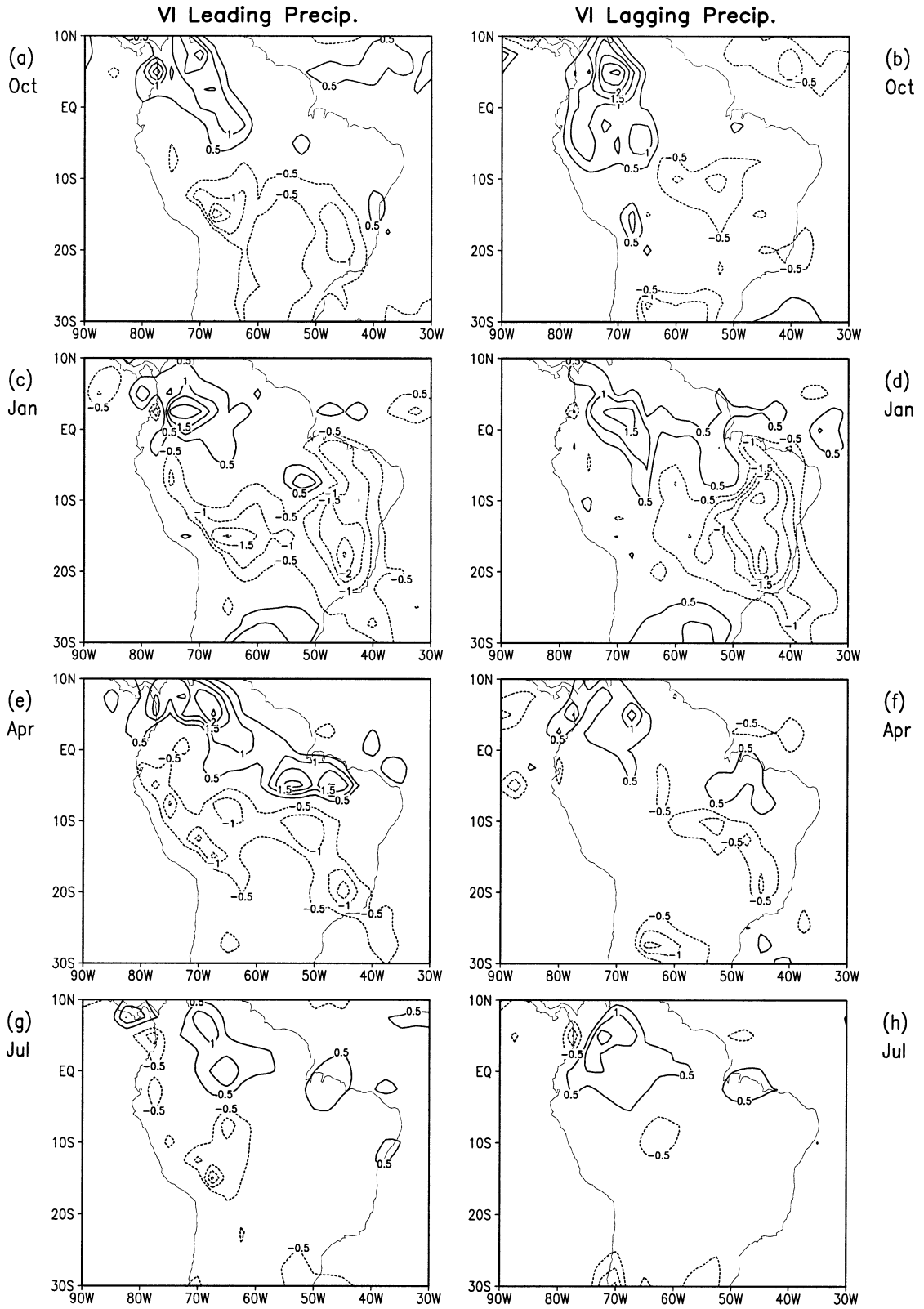

FIG. 12. Linear regression coefficient for (a),(b) Oct, (c),(d) Jan, (e),(f) Apr, and (g),(h) Jul daily precipitation associated with the 15-yr daily mean V index. (a),(c),(e),(g) and (b),(d),(f),(h) are shown for V index leading and lagging precipitation by 2 days, respectively. Contour interval is 0.5 mm day^{-1} (m s^{-1})$^{-1}$, with negative values dashed. Zero contours are omitted.

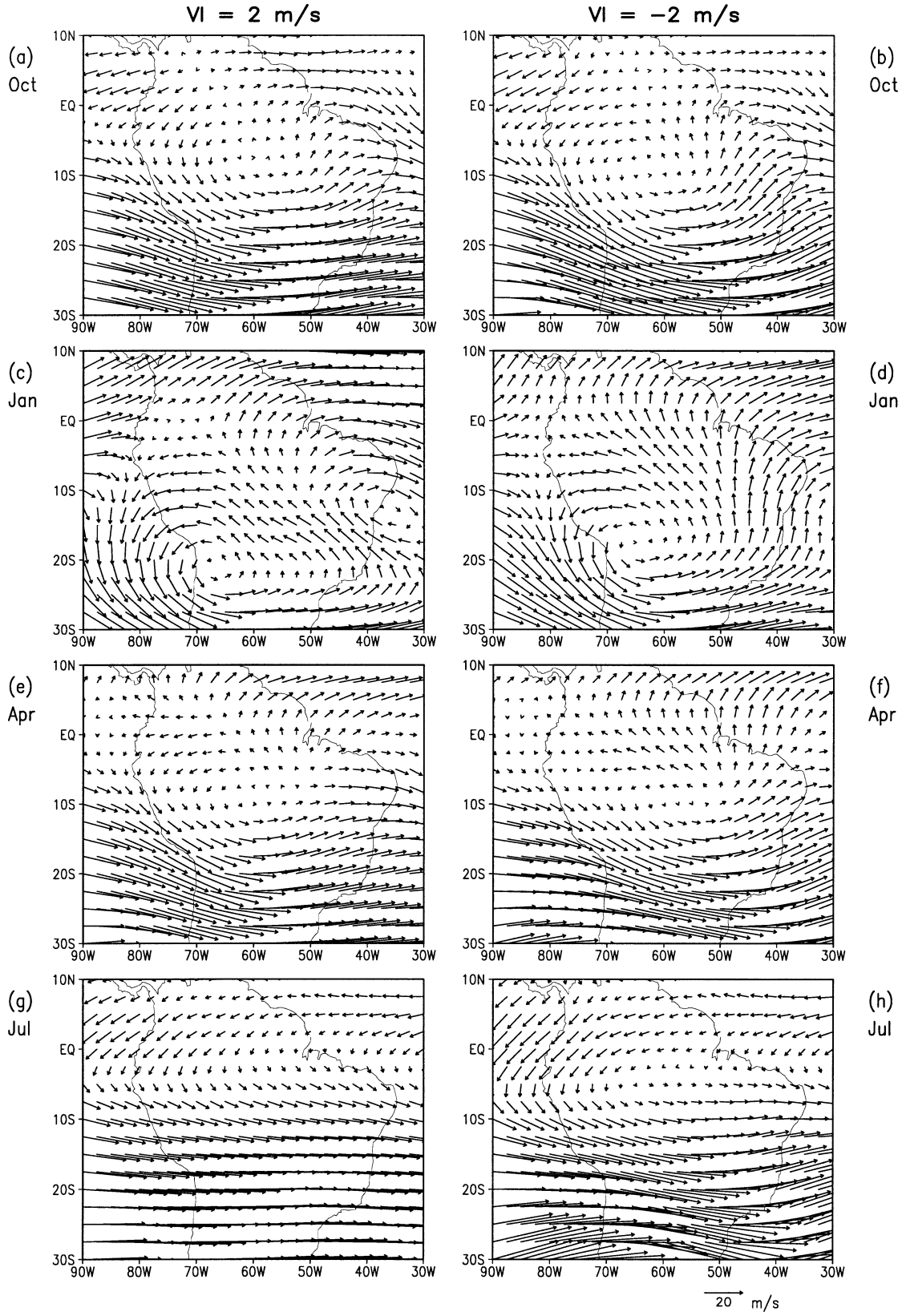

FIG. 13. As in Fig. 11, but for 200-hPa winds.

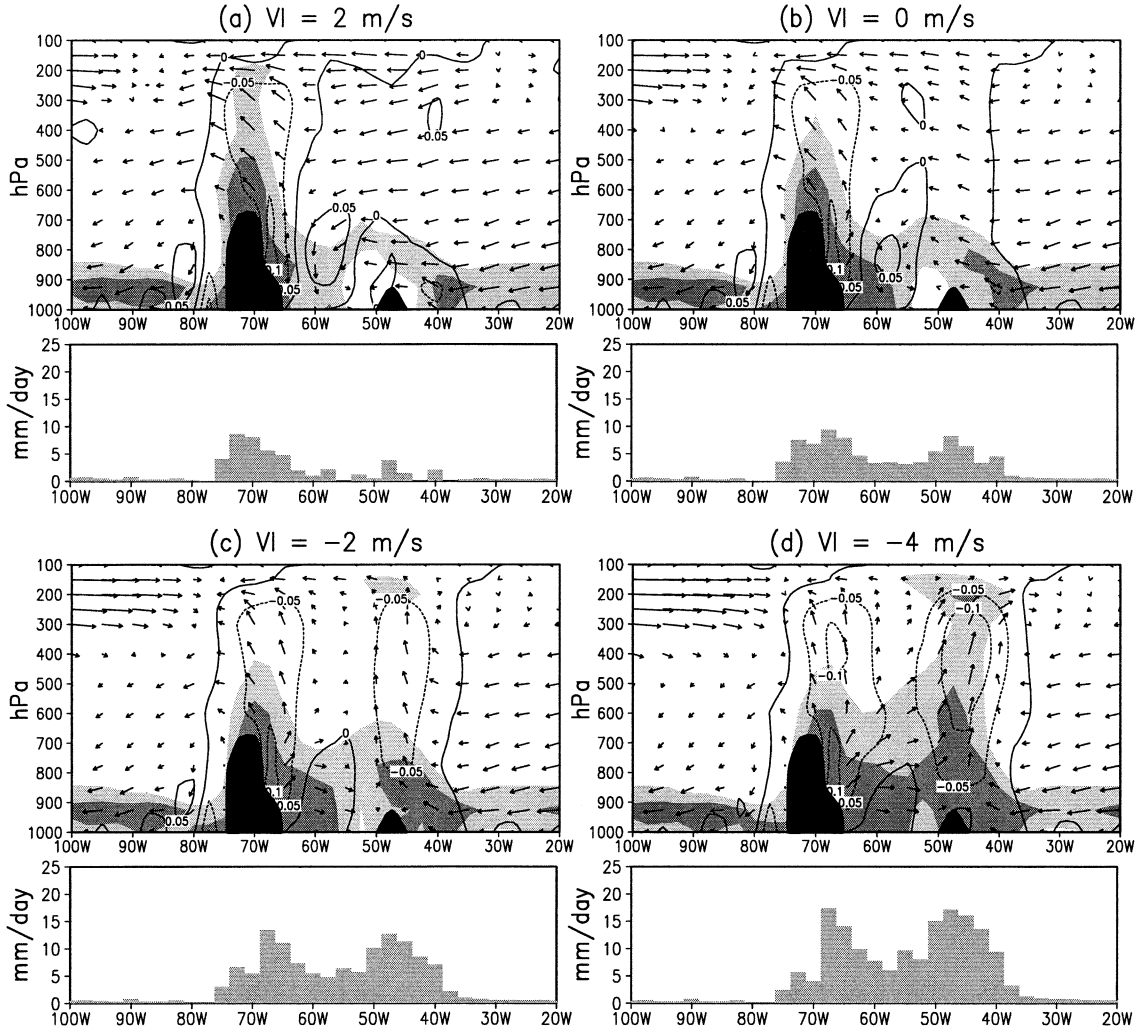

FIG. 14. Vertical cross section of wind (vectors), vertical velocity (dp/dt, contours), relative humidity (shadings), and precipitation (mm day^{-1}, bars) at 15°S, obtained using the linear regression against the 15-yr daily V index in Jan. Contour interval is Pa s^{-1}, with negative values (upward motion) dashed. Light and dark shadings indicate the relative humidity greater than 70% and 80%, respectively. Black shadings are topography.

This is also evident in Figs. 11c, 11d, and 14. Therefore, both the cross-equatorial flow and the subtropical zonal wind appear to relate to the similar large-scale circulation patterns. In relation to the seasonal variation of precipitation, however, the cross-equatorial flow may be more closely related to the basin-scale precipitation change, as it links to the source of the unstable air over the equatorial Atlantic Ocean. For example, although easterly winds show up near Rondonia in the southerly regime (Figs. 11a,c,e,g) the direction of zonal wind is not very clear in the northerly regime (Figs. 11b,d,f,h). It is also interesting that unlike its seasonal variation on a global scale (Fig. 7a), the submonthly fluctuations in the cross-equatorial flow have a very localized feature (Fig. 15a). This may indicate different forcing mechanisms responsible for the variations of the V index on different timescales.

6. Conclusions

Based on area-averaged daily mean 925-hPa meridional winds from 1979 to 1993, we constructed a meridional wind index, the V index, to examine the variability of the cross-equatorial wind over the equatorial western Amazon. Two atmospheric circulation regimes are identified, that is, a southerly regime and a northerly regime. The alternating southerly and northerly wind events exhibit large seasonal and submonthly variabilities, as well as interannual variability. The cross-equatorial wind is dominated by the southerly regime in the austral winter and by the northerly regime in summer. There is a transition from the southerly regime to the northerly regime in spring. It is demonstrated that, in each season, the spatial patterns of precipitation over South America are significantly different in the two cir-

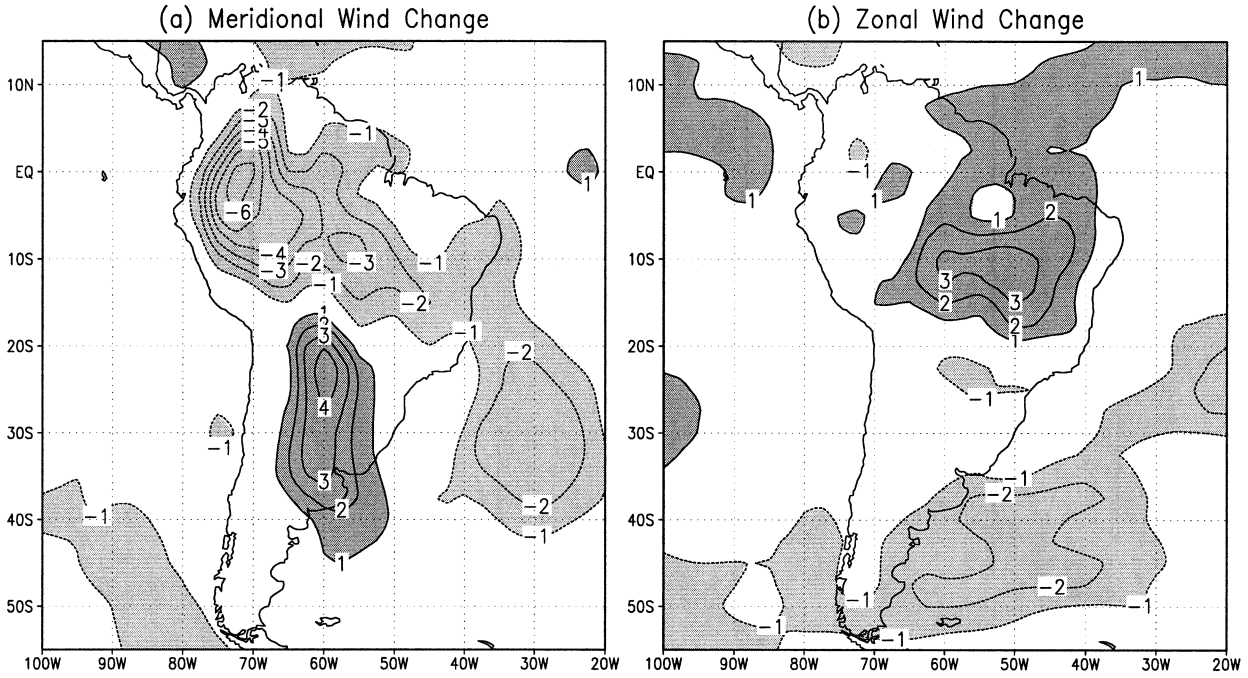

FIG. 15. 925-hPa (a) meridional and (b) zonal wind changes corresponding to a shift in the V index from 2 to −2 m s^{-1}, based on the linear regression. Contour interval is 1 m s^{-1}, with negative values dashed. Zero contours are omitted. Dark (light) shading indicates positive (negative) wind anomaly exceeding 1 m s^{-1}.

culation regimes. In general, associated with the southerly flow, precipitation is located to the north of the equator. In the northerly regime, precipitation is shifted toward the Amazon basin and the subtropics. The seasonal variations of South American precipitation, as well as the onset of the Amazon rainy season, are strongly related to the changes in direction of the cross-equatorial flow over the western Amazon and the frequency of these southerly and northerly wind events. The relation between the V index and 200-hPa circulation is consistent with the seasonal cycle of the South American monsoon circulation. The cross-equatorial flow is thus a good indicator for precipitation changes over tropical and subtropical South America.

The SVD analysis is applied to the 15-yr monthly mean precipitation and 925-hPa meridional winds over South America to identify the main contributing modes and related processes. The first SVD mode captures the precipitation variability on both sides of the equator that is linked to the seasonal migration of the Hadley circulation. The second SVD mode represents the precipitation changes over the equatorial eastern Amazon related to the Pacific and Atlantic SST variation. The first mode is dominant in winter and summer, while the second mode is dominant in spring and fall. The result in the first SVD mode is consistent with the relation between precipitation and the V index on the seasonal timescale. It is also suggested that the change in the cross-equatorial flow leads the variation of precipitation over South America.

Although the precipitation changes associated with the V index are similar on both seasonal and submonthly timescales, the processes responsible for the V index changes may be different between these two timescales. The seasonal variation of the V index, together with the Hadley circulation on a global scale, is driven by the seasonal change in solar insolation. On submonthly timescales, however, the fluctuations in the V index display a localized feature and may be attributable to various mechanisms. For example, during winter when southerly winds prevail over the equatorial western Amazon, Cohen et al. (1995) have shown that a northerly flow may occur when tropical easterly waves propagate from the Atlantic to the northern coast of South America. Thus, short-term fluctuations in the V index may be caused by easterly waves, which originate from Africa. Nogues-Paegle and Mo (1997) found that the intensity of SACZ could strongly influence the warm season precipitation over South America. This study shows that there are significant differences in the subtropical anticyclonic circulation over the SACZ region associated with the southerly and northerly regimes, not only in summer but also in other seasons. How the V index is related to the variation of SACZ needs to be further investigated.

This study emphasizes the relationship between South American precipitation and low-level meridional wind over the equatorial western Amazon. The precipitation is also strongly influenced by subtropical LLJs (Paegle 1998) and cold air incursions associated with fronts

(e.g., Marengo et al. 1997). Although we found some correlations between cross-equatorial flow and the strength and location of the LLJ, the subtropical LLJ has its own variability. The circulation pattern associated with cold air incursions does not show up in our composite analysis. These variabilities are largely independent of the V index and need to be examined in terms of their contributions to the precipitation variability.

Acknowledgments. This study was supported by the NOAA Pan American Climate Studies (PACS) program. We thank Drs. Pedro L. Silva Dias, Dana E. Hartley, and Walter A. Petersen for their enlightening discussion, and two anonymous reviewers for constructive comments. We also thank Ms. Mingxuan Chen for access to the ECMWF reanalysis data, and Ms. Margaret Sanderson Rae for editorial assistance.

REFERENCES

Bretherton, C. S., C. Smith, and J. M. Wallace, 1992: An intercomparison of methods for finding coupled patterns in climate data. *J. Climate,* **5,** 541–560.

Cohen, J. C. P., M. A. F. Silva Dias, and C. A. Nobre, 1995: Environmental conditions associated with Amazonian squall lines: A case study. *Mon. Wea. Rev.,* **123,** 3163–3174.

Fu, R., B. Zhu, and R. E. Dickinson, 1999: How do atmosphere and land surface influence seasonal changes of convection in the tropical Amazon? *J. Climate,* **12,** 1306–1321.

——, R. E. Dickinson, M. Chen, and H. Wang, 2001: How do tropical sea surface temperatures influence the seasonal distribution of precipitation in the equatorial Amazon? *J. Climate,* **14,** 4003–4026.

Gan, M. A., and V. B. Rao, 1991: Surface cyclogenesis over South America. *Mon. Wea. Rev.,* **119,** 1293–1302.

Garreaud, R. D., and J. M. Wallace, 1998: Summertime incursions of midlatitude air into subtropical and tropical South America. *Mon. Wea. Rev.,* **126,** 2713–2733.

Greco, S., and Coauthors, 1990: Rainfall and surface kinematic conditions over central Amazonia during ABLE 2B. *J. Geophys. Res.,* **95,** 17 001–17 014.

Horel, J. D., A. N. Hahmann, and J. E. Geisler, 1989: An investigation of the annual cycle of convection activity over the tropical Americas. *J. Climate,* **2,** 1388–1403.

Kousky, V. E., 1988: Pentad outgoing longwave radiation climatology for the South American sector. *Rev. Bras. Meteor.,* **3,** 217–231.

——, and M. T. Kayano, 1994: Principal modes of outgoing longwave radiation and 250-mb circulation for the South American sector. *J. Climate,* **7,** 1131–1143.

Krishnamurti, T. N., M. C. Sinha, B. Jha, and U. C. Mohanty, 1998: A study of South Asian monsoon energetics. *J. Atmos. Sci.,* **55,** 2530–2548.

Liebmann, B., G. N. Kiladis, J. A. Marengo, T. Ambrizzi, and J. D. Glick, 1999: Submonthly convective variability over South America and the South Atlantic convergence zone. *J. Climate,* **12,** 1877–1891.

Lu, E., and J. C. L. Chan, 1999: A unified monsoon index for south China. *J. Climate,* **12,** 2375–2385.

Marengo, J., A. Cornejo, P. Satyamurty, and C. Nober, 1997: Cold surges in tropical and extratropical South America: The strong event in June 1994. *Mon. Wea. Rev.,* **125,** 2759–2786.

——, B. Liebmann, V. E. Kousky, N. P. Filizola, and I. C. Wainer, 2001: Onset and end of the rainy season in the Brazilian Amazon basin. *J. Climate,* **14,** 833–852.

Nogues-Paegle, J., and K. C. Mo, 1997: Alternating wet and dry conditions over South America during summer. *Mon. Wea. Rev.,* **125,** 279–291.

Paegle, J., 1998: A comparative review of South America low-level jets. *Meteorologica,* **23,** 73–81.

Park, C.-K., and S. D. Schubert, 1993: Remotely forced intraseasonal oscillations over the tropical Atlantic. *J. Atmos. Sci.,* **50,** 89–103.

Petersen, W. A., S. W. Nesbitt, R. J. Blakeslee, R. Cifelli, P. Hein, and S. A. Rutledge, 2002: TRMM observations of intraseasonal variability in/over the Amazon. *J. Climate,* **15,** 1278–1294.

Rickenbach, T. M., R. N. Ferreira, J. Halverson, D. L. Herdies, and M. A. F. Silva Dias, 2002: Modulation of convection in the southwestern Amazon basin by extratropical stationary fronts. *J. Geophys. Res.,* in press.

Smith, T. M., R. W. Reynolds, R. E. Livezey, and D. C. Stokes, 1996: Reconstruction of historical sea surface temperature using empirical orthogonal functions. *J. Climate,* **9,** 1403–1420.

Stensrud, D. J., 1996: Importance of low-level jets to climate: A review. *J. Climate,* **9,** 1698–1711.

Velasco, I., and J. M. Fritsch, 1987: Mesoscale convective complexes in the Americas. *J. Geophys. Res.,* **92,** 9591–9613.

Wallace, J. M., C. Smith, and C. S. Bretherton, 1992: Singular value decomposition of wintertime sea surface temperature and 500-mb height anomalies. *J. Climate,* **5,** 561–576.

Zhou, J., and K.-M. Lau, 1998: Does a monsoon climate exist over South America? *J. Climate,* **11,** 1020–1040.